

A 0.1 - 50 GHz SiGe HBT Distributed Amplifier Employing Constant-k m-Derived Sections

Jorge Aguirre, Calvin Plett

Department of Electronics, Carleton University, Ottawa, Ontario, K1S 5B6, Canada

Abstract — This paper describes a single-ended three-stage SiGe HBT distributed amplifier employing constant-k, m-derived filter sections in the output artificial transmission line. The distributed amplifier exhibits a measured passband of 100 MHz to 50 GHz, has a small die size (1.0 x 1.1 mm²) and low power consumption (125 mW). This amplifier is suitable for use in communication systems.

I. INTRODUCTION

The telecommunications industry is focusing on wide bandwidth amplifiers for RF and fiber applications. Most manufacturers of 40 Gb/s components have obtained this wide bandwidth by using expensive technologies with high f_T . High speed circuits are being designed in SiGe with bit rates at or above 40 Gb/s, obtaining results previously only seen in the exotic III - V technologies [1] - [4]. The IBM BiCMOS SiGe process employed in the fabrication and design of this distributed amplifier reports an f_T of 120 GHz and an f_{max} of 100 GHz [5].

This paper describes a single-ended three-stage distributed amplifier useful for 40 Gb/s applications. The small die size (1.0 x 1.1 mm²) and fabrication in SiGe translates into low cost. The distributed amplifier has a low power consumption of 125 mW and a measured passband of 100 MHz to 50 GHz.

II. CIRCUIT DESIGN

The single-ended distributed amplifier is a 3-stage circuit (Fig. 1) that employs artificial input/output transmission lines.

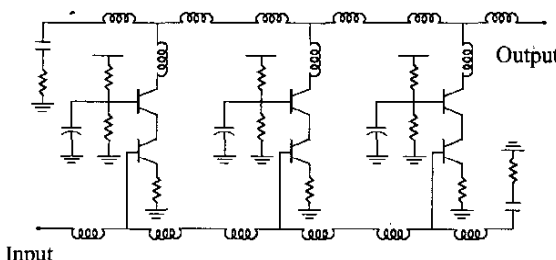


Fig. 1. Three-stage single-ended distributed amplifier

A. Artificial Transmission Lines

The two port networks of Fig. 2 are frequently used as simple models for lossless artificial transmission lines. [6] - [7].

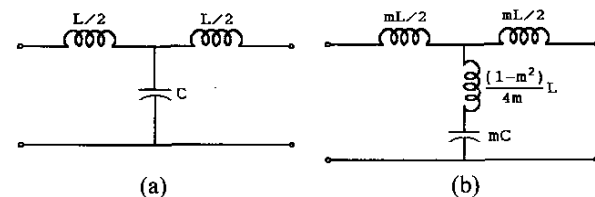


Fig. 2. (a) A constant-k T filter section, and (b) A constant-k m-derived T filter section

The constant-k filter section provides a means of connecting two gain stages without sacrificing gain bandwidth product. This is done by incorporating the device input and output capacitances of the individual gain stages into the filter section [6].

The constant-k section has an image impedance that is a function of frequency and is defined as:

$$Z_I = Z_O \sqrt{1 - \frac{\omega^2}{\omega_C^2}} \quad (1)$$

where the characteristic impedance is:

$$Z_O = \sqrt{\frac{L}{C}} = k \quad (2)$$

and the cutoff frequency is defined as:

$$\omega_C = \frac{2}{\sqrt{LC}} \quad (3)$$

This frequency dependant impedance defined by (1) is not physically realizable as a termination and so, often takes the form of a resistor with an impedance of Z_O . To improve the frequency response of the artificial transmission line a bisected m-derived filter section is often placed before the resistive termination. This section reduces the frequency dependence of the image impedance seen by the

resistive termination and as a result improves the performance of the artificial transmission line. Through careful design and the appropriate choice of filter section, the added complexity of incorporating the bisected m-derived filter sections into the artificial transmission line can be avoided.

The performance of the artificial transmission line is dependent on the type of filter sections used. Fig. 3. shows that the m-derived T section has a flatter passband and a better input reflection coefficient than its corresponding constant-k T section.

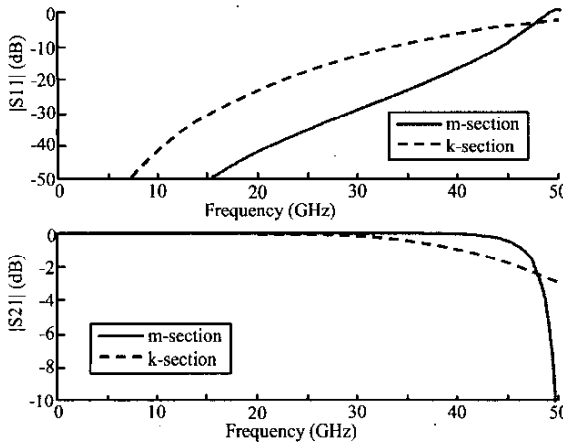


Fig. 3. $|S_{11}|$ and $|S_{21}|$ for the constant-k T section and m-derived T section, with $m = 0.1$.

The m-derived T section is a modification of the constant-k T section. Both sections still maintain the same image impedance as defined by (1) but the new m-section has an LC series resonance in the shunt arm. This resonance provides the ability to modify the passband attenuation. The resonant frequency of the LC shunt arm is defined as:

$$\omega_R = \frac{\omega_C}{\sqrt{1-m^2}} \quad (4)$$

where $0 < m < 1$. Note: if m is set to 1, the passband characteristics are identical to those of the constant-k - T section.

An artificial transmission line composed of m-derived sections is ideal for a distributed amplifier. However, there is a draw back. The m-derived sections take up more layout area. The choice then becomes a trade off between desired (or required) performance and the available die space. Therefore, the m-derived filter sections should be employed where better performance from the artificial transmission line is needed. The distributed amplifier presented here uses m-derived filter sections for the output

artificial transmission line and constant-k T sections for the input line (Fig. 1.).

B. Gain

A cascode design was chosen for the individual gain cells (Fig. 1) of the distributed amplifier. The addition of the cascode transistor reduces the Miller effect, and improves the isolation between the input and output artificial transmission lines. The reduction of the Miller effect coupled with the reduction in input capacitance brought about by the addition of the emitter resistor increases the upper frequency limit of the gain cell. The emitter degeneration resistor also helps reduce output distortion.

The voltage and power gain equations for the distributed amplifier assume: lossless artificial transmission lines, simplified transistor models, uniform current source excitation, input and output line phase synchronization and ideal terminations. The voltage gain is defined as:

$$A_V = \frac{-Ng_m}{2\sqrt{(1-\frac{\omega^2}{\omega_C^2}) + j\frac{\omega L_I}{R_{\pi 1} + R_E + g_m R_{\pi 1} R_E}}} Z_O e^{-N\theta} \quad (5)$$

And the power gain equation is:

$$G = \frac{N^2 g_m^2 Z_I Z_O}{4\sqrt{(1-\frac{\omega^2}{\omega_C^2}) + j\frac{\omega L_I}{R_{\pi 1} + R_E + g_m R_{\pi 1} R_E}}} e^{-2N\theta} \quad (6)$$

where N is the number of stages, g_m is the small signal transconductance of each stage, θ is the complex propagation constant of the line, Z_I and Z_O are the characteristic impedances of the input and output artificial transmission lines respectively, L_I is the inductance of the input constant-k T section, R_E is the emitter degeneration resistance and $R_{\pi 1}$ is the small signal π transistor model input resistance.

III. MEASURED CIRCUIT PERFORMANCE

The single-ended three-stage distributed amplifier (Fig. 4) employs off-chip 50 Ohm terminations for the dummy loads of the artificial transmission lines. Unfortunately, the electrical length introduced by the off-chip terminations was not taken into account and introduced multiple reflections throughout the passband. The output artificial transmission line $|S_{11}|$ was measured first with port 1 of the network analyzer and an off-chip termination for the dummy load and then with the termination replaced with port 2 of the network analyzer (Fig. 5 (a)). It can be clearly seen that the removal of the off-chip termination also removes the reflections. A comparison between the

measured $|S_{11}|$ and spline approximated reflection-free $|S_{11}|$ (Fig. 5 (b)) of the output artificial transmission line shows that the spline approximation is an adequate representation of the reflection-free frequency response. The spline approximation will be used for the S parameter and group delay plots.

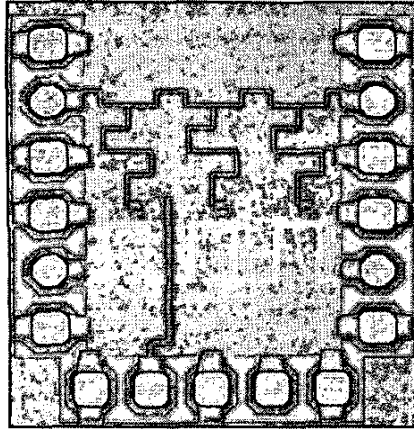


Fig. 4. Die photograph of the $1.0 \times 1.1 \text{ mm}^2$ three-stage single-ended distributed amplifier.

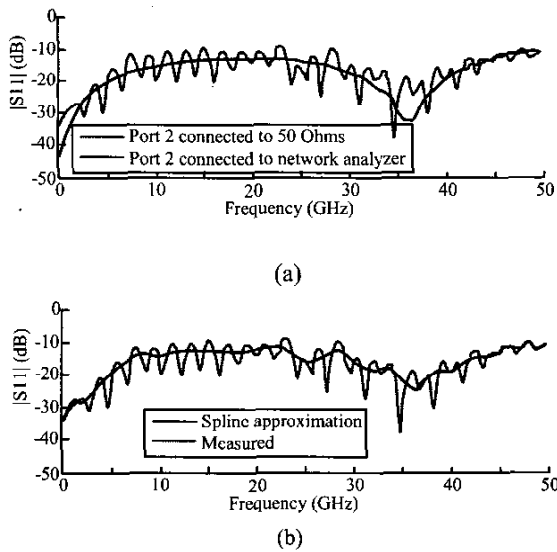


Fig. 5. A comparison of the measured $|S_{11}|$ of the output artificial transmission line (a) with a 50 Ohm dummy load termination and with the 50 Ohm termination replaced with port 2 of the network analyzer and (b) the spline approximation of $|S_{11}|$ and port 2 of the network analyzer as the dummy load.

The distributed amplifier simulations were done with the supplied IBM models and models created from simulations in Momentum and ADS. The S parameters were measured with a network analyzer and pico probe station. The network analyzer is limited to a maximum bandwidth of 50 GHz. The bandwidth can be seen to exceed 50 GHz for the distributed amplifier (Fig. 8). The amplifier exhibits a passband gain (measured from 100 MHz to 50 GHz) that varies from approximately 9 dB to 5 dB. The input reflection coefficient (Fig. 6) is better than -15 dB and the output reflection coefficient (Fig. 7) is better than -12 dB. The reverse transmission coefficient (Fig. 9) is less than -40 dB. The calculated group delay from measured and simulated S parameters (Fig. 10) is approximately 20 pS, relatively constant over the bandwidth. The distributed amplifier employs a 5V rail and dissipates 125 mW of power.

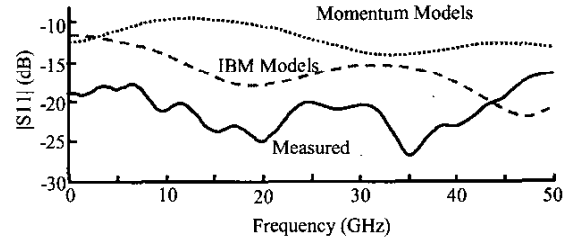


Fig. 6. Measured and simulated $|S_{11}|$

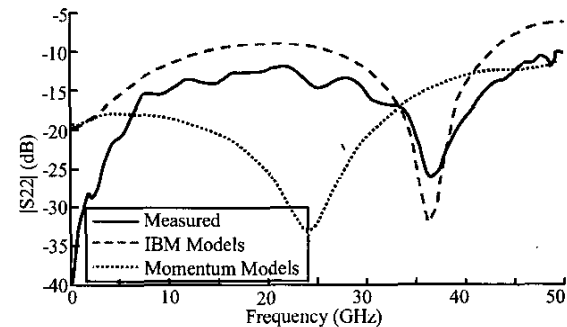


Fig. 7. Measured and simulated $|S_{22}|$

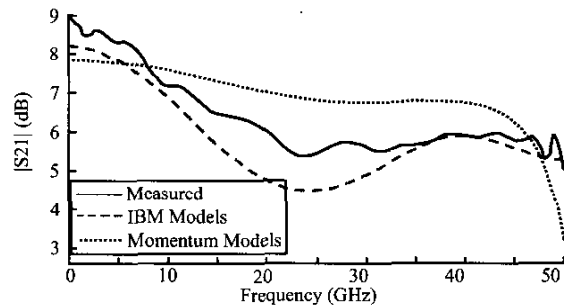


Fig. 8. Measured and simulated $|S_{21}|$

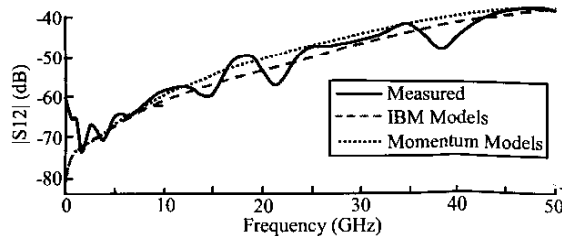


Fig. 9. Measured and simulated $|S_{12}|$

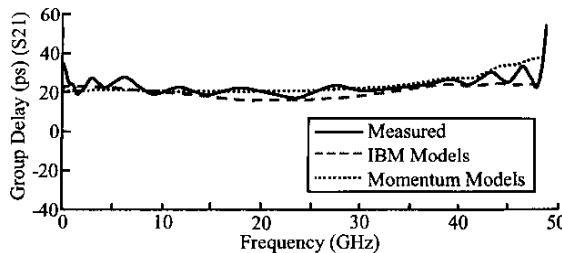


Fig. 10. Calculated Group delay from measured and simulated data.

The 1 dB compression point was measured and simulated for a few values of frequency (1, 10, 30, and 49 GHz). If operation across the entire bandwidth is desired then an input power limitation is approximately measured to be 0.84 dBm (Fig. 11). This is the upper limit of input power because it is the lowest measured 1 dB input referred compression point. The corresponding output power is 8.49 dBm (Fig. 11).

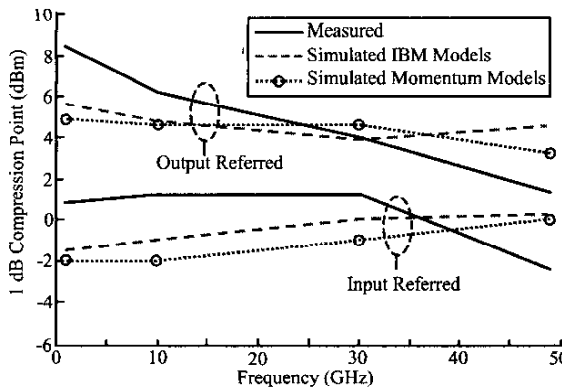


Fig. 11. The input and output referred 1 dB compression point.

IV. CONCLUSION

This paper presented a 0.1 - 50 GHz single-ended three-stage SiGe HBT distributed amplifier. With 9 - 5 dB gain, an input/output reflection coefficient better than -12 dB

and a reverse transmission coefficient better than -40 dB. The amplifier employed constant-k m-derived filter sections and constant-k T filter sections in the artificial transmission lines. The performance of the amplifier is dependant on the performance of the artificial transmission lines. It is clear that the constant-k m-derived filter sections can be employed when better performance is needed to obtain the desired (or required) results. The amplifier dissipates 125 mW of power and is only $1.0 \times 1.1 \text{ mm}^2$ in size, these factors coupled with the achieved results make the SiGe process a capable alternative to the more exotic III - V technologies for distributed amplification.

ACKNOWLEDGEMENT

The authors would like to thank Micronet for financial support and the Technology Access Group, Nortel Networks for access to the resources and people that helped in the design of this amplifier.

REFERENCES

- [1] J. Mullrich, W. Klein, R. Khelifi, and H. M. Rein, "SiGe regenerative frequency divider operating up to 63 GHz," *Electron. Lett.*, vol. 35, no. 20, pp. 1730 - 1731, Sept. 1999.
- [2] R. Schmid, T. F. Meister, M. Rest, and H. M. Rein, "40-Gb/s EAM driver IC in SiGe bipolar technology," *Electron. Lett.*, vol. 34, no 11, pp. 1095 - 1097, May 1998.
- [3] K. Ohhata, F. Arakawa, T. Masuda, N. Shiramizu, and K. Washio, "40-Gb/s analog IC chipset for optical receivers-AGC amplifier, full-wave rectifier and decision circuit-Implemented using self-aligned SiGe HBTs," in *IEEE MTT-S Int. Microwave Symp. Dig.*, vol. 3, pp. 1701 - 1704, May 2001.
- [4] T. Masuda, K. Ohhata, N. Shiramizu, E. Ohue, K. Oda, R. Hayami, H. Shimamoto, M. Kondo, T. Harada, and K. Washio, "40-Gb/s 4:1 multiplexer and 1:4 demultiplexer IC module using SiGe HBTs," in *IEEE MTT-S Int. Microwave Symp. Dig.*, vol. 3, pp. 1697 - 1700, May 2001.
- [5] A. Joseph, D. Coolbaugh, M. Zierak, R. Wuthrich, P. Geiss, Z. He, X. Liu, B. Orner, J. Johnson, G. Freeman, D. Ahlgren, B. Jagannathan, L. Lanzerotti, V. Ramachandran, and J. Malinowski, "A 0.18- μm BiCmos technology featuring 120/100 GHz (f/f_{\max}) HBT and ASIC-compatible CMOS using copper interconnect," in *Proc. IEEE BCTM*, pp. 143 - 146, 2001.
- [6] T. T. Y. Wong, *Fundamentals of Distributed Amplification*. Norwood MA: Artech, 1993.
- [7] D. M. Pozar, *Microwave Engineering second edition*. New York: John Wiley & Sons, Inc, 1998.